

Tryptanthrin-Loaded Nanoparticles for Delivery into Cultured Human Breast Cancer Cells, MCF7: the Effects of Solid Lipid/Liquid Lipid Ratios in the Inner Core

Yi-Ping FANG,^a Yin-Ku LIN,^{b,c} Yu-Han SU,^d and Jia-You FANG^{*,d,†}

^a Department of Biotechnology, Yuanpei University; Hsinchu 300, Taiwan; ^b Department of Traditional Chinese Medicine, Chang Gung Memorial Hospital; Keelung 204, Taiwan; ^c College of Medicine, Chang Gung University; and ^d Pharmaceuticals Laboratory, Graduate Institute of Natural Products, Chang Gung University; Kweishan, Taoyuan 333, Taiwan. Received October 5, 2010; accepted November 24, 2010; published online November 26, 2010

Tryptanthrin is an ancient medicine which recently was also found to have a function of downregulating multidrug resistance (MDR). However, tryptanthrin is insoluble in water, which limits its availability for delivery into cancer cells. There is a need to improve delivery systems to increase the inhibition of MDR. The aim of this study was to employ nanoparticles encapsulating tryptanthrin to improve the delivery and promote the sustained release of this drug. The approach was to encapsulate tryptanthrin in various nanoparticles, including solid lipid nanoparticles (SLNs), nanostructured lipid carriers (NLCs), and lipid emulsions (LEs). We compared the particle size and zeta potential of these nanoparticles, and evaluated the partitioning behavior of tryptanthrin in them. We also determined the release kinetics of tryptanthrin from these nanoparticles. Moreover, cellular cytotoxicity toward and uptake of tryptanthrin-loaded nanoparticles by human breast cancer cells were determined. We found that the mean particle size of NLCs was lower, and the partition coefficient was higher than those of SLNs, and an increased tryptanthrin release rate was found with the NLC delivery system. NLCs achieved the sustained release of tryptanthrin without an initial burst. In particular, the NLC-C formulation, composed of a mixture of Compritol and squalene as the core materials, showed the highest release rate and cytotoxic effect. Confocal laser scanning microscopic images confirmed drug internalization into cells which enhanced the endocytosis of the particles. These results suggested that NLCs can potentially be exploited as a drug carrier for topical or intravenous use in the future.

Key words solid lipid nanoparticle; nanostructured lipid carrier; tryptanthrin; delivery; human breast cancer cell; multidrug resistance

Chemotherapeutics are the mainstream strategy for clinically treating cancers. However, the therapeutic effects of anticancer drugs are obstructed by multidrug resistance (MDR) which is an important issue of concern related to the success of chemotherapy.¹⁾ Much research is being devoted to elucidating the mechanisms of MDR in the ATP-binding cassette (ABC) family, which actively transports proteins, to overcome this problem. MDR can be caused by the transport of proteins of ATP-binding drugs out of cells, thereby resulting in a decrease in the intracellular drug concentration.²⁾ ABC transport is divided into many types, and the first identified was the P-glycoprotein (P-gp, also called MDR1), which plays a particular role in regulating MDR1 gene expression.³⁾

Tryptanthrin is an ancient traditional folk medicine derived from *Polygonum tinctoriu*, a member of the indigo plant family.⁴⁾ Tryptanthrin can also be produced by *Candida lipolytica* when grown in media containing an excess of tryptophan, hence the name tryptanthrin.⁵⁾ This compound is used to treat microbial infections, inflammation, clotting disorders, and various cancers.^{6–8)} In addition, recent studies showed that tryptanthrin downregulates MDR-associated protein (MRP) gene expression and is a potential anticancer drug.⁹⁾ Since tryptanthrin is a planer tetracyclic structure, it can interact with DNA through π - π stacking and hydrogen bonding. Furthermore, the alkylamine moiety of tryptanthrin allows for binding with the third oligonucleotide site in DNA via electrostatic interactions.⁴⁾ Accordingly, tryptanthrin may

be useful in treating certain cancers, in particular those that exhibit MDR. However, since tryptanthrin is insoluble in most biocompatible media, it is difficult to deliver into cancer cells using conventional application techniques, such as oral ingestion or an intravenous or intramuscular injection.¹⁰⁾

To date, many studies showed that nanoparticles can be used as carriers which can solve insolubility problems by delivering lipophilic compounds into cancer cells.¹¹⁾ In general, nanoparticles fall into one of two classes that differ from other traditional vehicles such as creams, tinctures, and lipid emulsions: solid lipid nanoparticles (SLNs) and nanostructured lipid carriers (NLCs).¹²⁾ Nanoparticle carriers provide for the controlled release of drugs; moreover, because the particle sizes are in nanoscale range, the efficacy of lipophilic compound delivery and bioavailability are increased.

In light of this background, we wanted to encapsulate tryptanthrin in lipid-based nanoparticles, and focused on comparing SLN-, NLC-, and lipid emulsion (LE)-based tryptanthrin carriers, with increased cancer cell permeation and controlled release properties for breast cancer cells. The applicability of those nanoparticles was demonstrated through extensive characterization of the particle size, charge, and release kinetics. In addition, these tryptanthrin-loaded lipid particles were used to treat cultured breast cancer cells, and the cellular cytotoxicity and uptake ability were evaluated.

Experimental

Materials Tryptanthrin was obtained from Wako Chemical (Osaka, Japan). Hydrogenated soybean phosphatidylcholine (SPC, Phospholipon

[†] Present address: Department of Cosmetic Science, Chang Gung Institute of Technology; Kweishan, Taoyuan 333, Taiwan.

80H) was obtained from American Lecithin (Woodside, NY, U.S.A.). Squalene was purchased from Sigma-Aldrich Chemical (St. Louis, MO, U.S.A.). Compritol 888 ATO and Precirol ATO 5 were purchased from Gattefossé (Gennevilliers, France). Sulforhodamine (SB) acid chloride was purchased from Fluka (Happague, NY, U.S.A.). Cellulose membranes (Cellu-Sep® T2, with a molecular weight cutoff of 6000–8000) were supplied by Membrane Filtration Products (Seguin, TX, U.S.A.). Other chemicals used in the study were of reagent grade. The human breast cancer cell line (MCF 7) was purchased from the Culture Collection and Research Center (CCRC) of the Food Industry Research and Development Institute (FIRDI, Hsinchu, Taiwan). Cell culture media and supplements were obtained from GIBCO Invitrogen (Grand Island, NY, U.S.A.).

Preparation of Lipid Nanoparticles Lipid nanoparticles were prepared according to the hot homogenization method. The lipid and aqueous phases were prepared separately. The lipid phase consisted of solid or liquid lipids and a lipophilic emulsifier (SPC), while the aqueous phase consisted of double-distilled water and a hydrophilic emulsifier (Tween 80). The two phases were heated separately to 85 °C for 15 min. The aqueous phase was added to the lipid phase and mixed using a high-shear homogenizer (Pro 250, Pro Scientific, Monroe, CT, U.S.A.) for 5 min. The mixture was further treated using a probe-type sonicator (VCX600, Sonics and Materials, Newtown, CT, U.S.A.) for 10 min at 85 °C. The total volume of the final product was 10 ml. The composition of the lipid nanoparticle systems (SLNs, NLCs, and LEs) are demonstrated in Table 1.

Vesicle Size and Zeta Potential The particle size and zeta potential were measured by laser light-scattering (LLS) with a helium–neon laser at 630 nm (ZS 90, Malvern, Worcestershire, U.K.). All particle systems were diluted 100-fold with deionized water before the size and zeta potential measurements. The determination was repeated three times per sample for three samples. All particle sizes and zeta potentials were measured at 25 °C.

Partition Behavior of Tryptanthrin in Various Lipid Nanoparticles Tryptanthrin (3 mg) was dissolved in a test tube containing acetonitrile (10 ml), and the organic solvent was removed by a vacuum evaporator. Then a mixture of melted lipid (1 g) and 1 ml of hot distilled water was dispersed in the test tube, and shaken for 30 min in a hot-water bath (85 °C). The aqueous and oil phases were separated after cooling by ultracentrifugation (Beckman Coulter Allegra™ 21R centrifuge, Fullerton, CA, U.S.A.) at 5445×g for 10 min. The aqueous phase was sampled with a syringe and filtered through a 0.45- μ m polyvinylidene difluoride (PVDF) filter. Concentrations of tryptanthrin were determined by high-performance liquid chromatography (HPLC). The partition coefficient ($\log P_{\text{octanol/water}}$) was calculated by the following equation:

$$\log P_{\text{oil/water}} = \log C_{\text{oil}}/C_{\text{water}}$$

where C_{oil} is the tryptanthrin concentration in the oil phase and C_{water} is the tryptanthrin concentration in the water phase.

In Vitro Tryptanthrin Release Kinetics from Various Lipid Nanoparticles Tryptanthrin release from the nanoparticles was measured using a Franz diffusion cell (Ching Fa, HsinChu, Taiwan). A cellulose membrane was mounted between the donor and receptor compartments. The membrane was soaked in double-distilled water for 12 h before mounting in the Franz diffusion cell. The donor medium consisted of 0.5 ml of vehicle containing tryptanthrin nanoparticle or a control solution (2.3 mmol/l tryptanthrin in dimethyl sulfoxide (DMSO)). The receptor medium consisted of 5.5 ml of 50% ethanol in pH 7.4 buffer to maintain sink conditions during the experiments. The available diffusion area between the cells was 0.785 cm². The stirring rate and temperature were kept at 600 rpm and 37 °C, respectively. At appropriate intervals, 300 μ l aliquots of the receptor medium were with-

drawn and immediately replaced with an equal volume of fresh buffer. The released amount of drug was determined by HPLC.

HPLC Analysis of Tryptanthrin Tryptanthrin was analyzed with an HPLC system consisting of a Hitachi L-2130 pump, a Hitachi L-2200 sample processor, and a Hitachi L-2400 UV detector (Tokyo, Japan). A reverse-phase column (Lichrospher RP-18, 250×4 mm, 5 μ m, Merck, Darmstadt, Germany) was used. The mobile phase was acetonitrile : water (55 : 45) adjusted with formic acid to pH 2.5 at a flow rate of 1 ml/min. The UV wavelength was set to 250 nm.

In Vitro Cellular Cytotoxicity Test Cellular cytotoxicity was determined by a 3-(4,5-dimethylthiazol-2-yl)-2,5-diphenyltetrazoleum bromide (MTT) assay. Human breast cancer cells (MCF-7) were grown in Dulbecco's modified Eagle's medium (DMEM) with 10% fetal bovine serum (FBS) and 1% antibiotics at 37 °C in a humidified atmosphere containing 5% CO₂. MCF-7 cells at 1×10⁴ cells/well were seeded in 24-well plates. Tryptanthrin or tryptanthrin encapsulated in various lipid nanoparticles (2.5 μ l) was added and incubated for 24 and 48 h. After washing with phosphate-buffered saline (PBS), cells were incubated with an MTT solution (50 mg/ml) in DMEM for 4 h. Formazan crystals resulting from MTT reduction were dissolved by adding 400 μ l DMSO for 30 min. The quantity of surviving cells was measured by an enzyme-linked immunosorbent assay (ELISA) reader at 550 nm.

Cell Uptake of Lipid Nanoparticles by Confocal Laser Scanning Microscopic (CLSM) Observations SB was loaded in the lipid nanoparticles using the same preparation procedure as described for preparing the lipid nanoparticles. MCF-7 cells at 1×10⁴ cells/well were seeded in 24-well plates, and sulforhodamine B-labeled nanoparticles or the control DMSO solution were added for 24 h in an incubator. Subsequently, MCF-7 cells were examined with a CLSM (Radiance 2100, Bio-Rad, Hercules, CA, U.S.A.). Optical excitation was carried out with a 543-nm He–Ne laser beam, and the fluorescence emission was detected at 590 nm.

Statistical Analysis Data are expressed as the mean±S.D. Statistical analyses were performed using unpaired Student's *t*-test with WINKS version software. A 0.05 level of probability was used as the level of significance. An analysis of variance (ANOVA) test was also used.

Results

Characterization of Various Lipid Nanoparticles (SLNs, NLCs, and LEs) We evaluated the characteristics of these tryptanthrin-loaded lipid particles. The lipid nanoparticle systems consisted of a lipid phase (solid and liquid lipids), water phase, and lipid/water interphase. The compositions of the SLNs, NLCs, and LEs are given in Table 1. The nanoparticles were developed by hot homogenization followed by ultrasonication to prepare three kinds lipid nanoparticles. In the tryptanthrin-loaded mixtures, we observed no distinct, undissolved crystals. Table 2 summarizes the particle size and zeta potential of the lipid nanoparticles. The SLN and NLC systems had particle sizes in the ranges of 320–653 and 198–269 nm, respectively. In general, the particle sizes of the different formulations of lipid nanoparticles decreased in the order of SLNs>LEs>NLCs. In addition, SLNs and NLCs were made of Precirol or Compritol as the core material. We observed that the lipid nanoparticles

Table 1. The Composition of the Nano-carriers System (SLN, NLC, LE)

Formulation code	Solid lipid (%, w/v)	Liquid lipid (%, w/v)	Lipophilic emulsifier (%, w/v)	Hydrophilic emulsifier (%, w/v)
SLN-P	Precirol (12)	—	SPC (0.2)	Tween 80 (2.4)
SLN-C	Compritol (12)	—	SPC (0.2)	Tween 80 (2.4)
SLN-M	Precirol (6) Compritol (6)	—	SPC (0.2)	Tween 80 (2.4)
NLC-P	Precirol (6)	Squalene (6)	SPC (0.2)	Tween 80 (2.4)
NLC-C	Compritol (6)	Squalene (6)	SPC (0.2)	Tween 80 (2.4)
LE	—	Squalene (12)	SPC (0.2)	Tween 80 (2.4)

SLN, solid lipid nanoparticles; NLC, nanostructured lipid carriers; LE, lipid emulsion; P, precirol; C, compritol; M, mixture of precirol and compritol; SPC, soybean phosphatidylcholine.

incorporating Precirol were smaller than those using Compritol ($p < 0.05$).

Partitioning Behavior of Tryptanthrin in Various Lipid Nanoparticles In order to understand the partitioning behavior of tryptanthrin in different lipid nanoparticles, we determined the tryptanthrin concentration in the aqueous phase, and calculated the partition coefficients ($\log P$ =ratio of the amount of tryptanthrin in the lipid phase to that in the aqueous phase). The results are shown in Table 3. In general, the partitioning ability of these lipid nanoparticles in NLCs were higher than in SLNs; moreover, when incorporated with Precirol, the ability was higher than that with Compritol.

Release Kinetics of Tryptanthrin from Various Nanoparticles We measured the accumulative amount of

tryptanthrin in the receptor compartment and calculated the parameters of the release kinetics from the three kinds of nanoparticles to explore the release behavior. Table 3 summarizes the accumulative amounts and release rates of tryptanthrin from SLNs, NLCs, and LEs. Since tryptanthrin is hydrophobic, DMSO was used as the solvent in the control group. In general, the release rate of the different types of nanoparticles decreased in the order of control > NLCs > LEs > SLNs. The release kinetics of various nanoparticles was fitted with a zero-order model. As shown in Fig. 1, the control group showed more-rapid release behavior (about 60% of the drug was released within 48 h) compared to the other nanoparticles. Moreover, all of the nanoparticles showed high sustained release trends, with 30% of the total drug amount released within 48 h for SLNs, and 36–45% for NLCs and LEs.

Cytotoxicity against Breast Cancer Cells In order to assess the cytotoxicity of the three kinds of nanoparticles, we used breast cancer cells (MCF-7) to examine cell viability (Fig. 2). Tryptanthrin was dissolved in DMSO as the control group. The viability levels of breast cancer cells treated with

Table 2. The Characterization of SLN, NLC, and Lipid Emulsion by Particle Size and Zeta Potential

Formulation	Particle size (nm)	Zeta potential (mV)
SLN-P	320.39 ± 21.02	-27.22 ± 4.66
SLN-C	539.67 ± 6.62	-32.77 ± 0.78
SLN-M	653.62 ± 56.21	-34.52 ± 6.20
NLC-P	198.45 ± 1.53*	-37.72 ± 8.70
NLC-C	269.50 ± 29.71*	-30.12 ± 3.08
LE	303.05 ± 62.10	-35.78 ± 2.77

* $p < 0.05$ different from respective SLN systems. Each value represents the mean ± S.D. ($n = 3$).

Table 3. The Characterization of SLN, NLC, and Lipid Emulsion by $\log P$ and Release Rate

Formulation	Log P (oil/water)	Accumulative amount ($\mu\text{g}/\text{cm}^2$)	Release rate ($\mu\text{g}/\text{cm}^2/\text{h}$)
Control	—	217.86 ± 16.02	16.62 ± 0.90
SLN-P	1.78 ± 0.04	86.75 ± 4.89	7.35 ± 0.40
SLN-C	1.53 ± 0.05	100.82 ± 5.48	8.69 ± 0.54
SLN-M	1.69 ± 0.03	84.32 ± 7.58	6.99 ± 0.44
NLC-P	1.91 ± 0.05	133.21 ± 3.84*	14.16 ± 0.39*
NLC-C	1.79 ± 0.07	166.52 ± 10.87*	14.62 ± 0.87*
LE	1.87 ± 0.05	136.93 ± 8.51	11.61 ± 0.65

* $p < 0.05$ different from respective SLN systems. Each value represents the mean ± S.D. ($n = 4$).

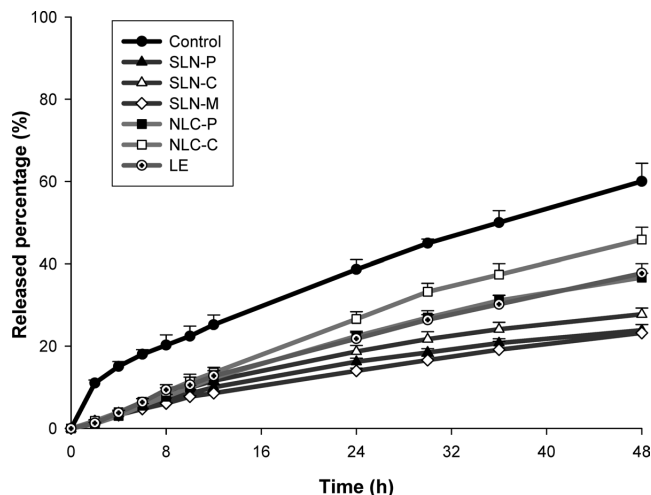
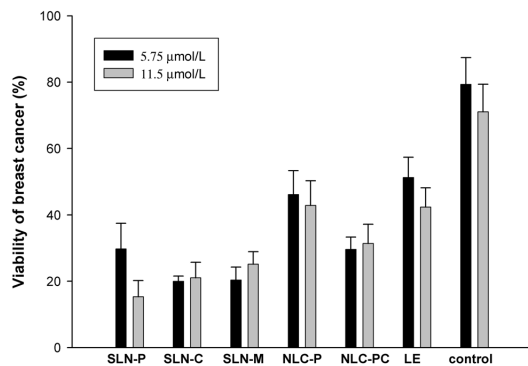


Fig. 1. *In Vitro* Release of Tryptanthrin across a Cellulose Membrane from Control Solution (Tryptanthrin 2.3 mmol/l) and Various Lipid Nanoparticles Systems

Each value represents the mean ± S.D. ($n = 4$).

(A) 24 h



(B) 48h

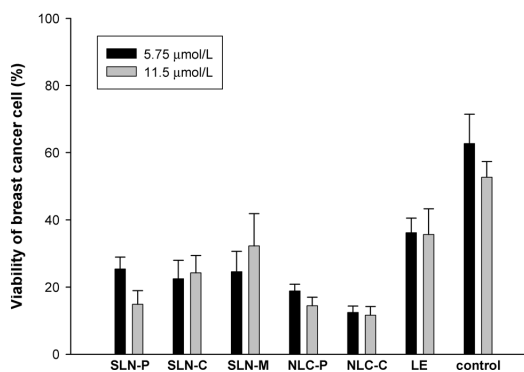


Fig. 2. Viability of Breast Cancer Cells (MCF-7) Following Treatment with Tryptanthrin (5.6 $\mu\text{mol}/\text{l}$ and 11.5 $\mu\text{mol}/\text{l}$) in Control Solution or Nanostructured Lipid Carriers after Incubation of 24 h (A) and 48 h (B)

Each value represents the mean ± S.D. ($n = 4$).

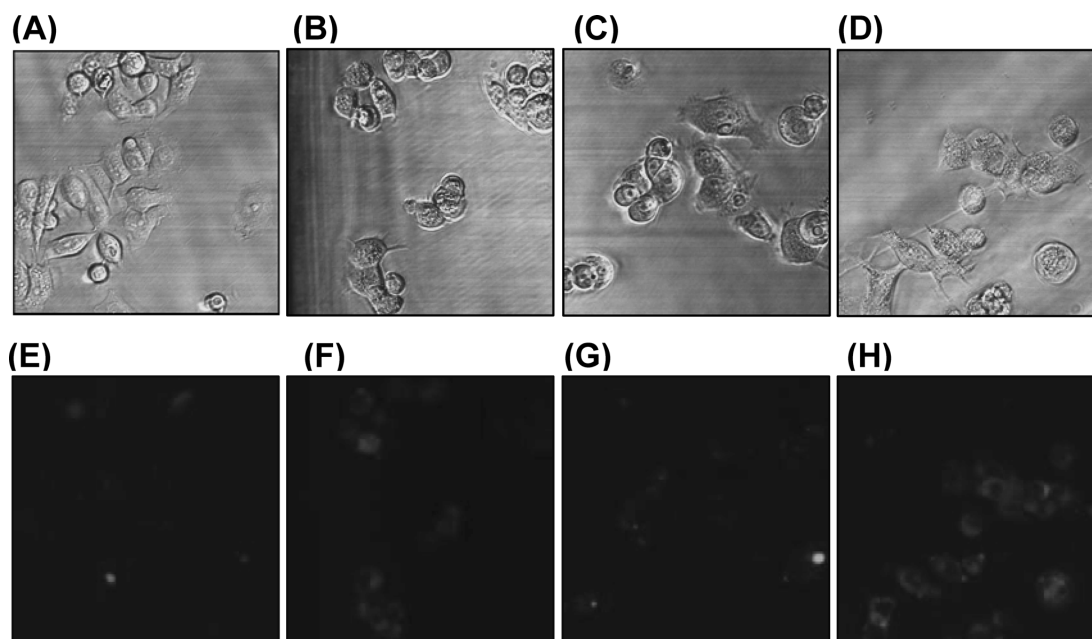


Fig. 3. The Confocal Laser Scanning Microscopic Images of Uptake of Sulforhodamine B-Labeled NLC-C by Breast Cancer Cells (CLSM, $\times 900$)

The breast cancer cells observed under a white light treated by (A) control solution ($5.2 \mu\text{mol/l}$ SB), (B) NLC-C ($5.2 \mu\text{mol/l}$ SB), (C) control solution ($10.4 \mu\text{mol/l}$ SB), and (D) NLC-C ($10.4 \mu\text{mol/l}$ SB). The breast cancer cells observed under a He-Ne laser beam treated by (E) control solution ($5.2 \mu\text{mol/l}$ SB), (F) NLC-C ($5.2 \mu\text{mol/l}$ SB), (G) control solution ($10.4 \mu\text{mol/l}$ SB), and (H) NLC-C ($10.4 \mu\text{mol/l}$ SB). SB, Sulforhodamine B acid chloride.

free drug in DMSO at low ($5.75 \mu\text{mol/l}$) and high concentrations ($11.5 \mu\text{mol/l}$) were 71–79% and 52%–62%, respectively. In general, the viability of these nanoparticles at $5.75 \mu\text{mol/l}$ decreased in the order of the control > LEs > NLCs > SLNs at 24 h; and the control > LEs > SLNs > NLCs at 48 h. Moreover, regardless of whether at 24 or 48 h, when incorporated with Precirol, the cell viability was higher than that with Compritol in the NLC group. On the other hand, at $11.5 \mu\text{mol/l}$, all of the nanoparticles showed decreased cell viability ($p > 0.05$) following an increase in the tryptanthrin concentration, except NLC-P and SLN-P ($p < 0.05$).

Cellular Uptake Ability According to CLSM Studies

To determine whether the nanoparticles were internalized by tumor cells, the uptake levels of SB-labeled nanoparticles and free SB in the aqueous solution (control) were examined. We used potential nanoparticles (NLC-C) to confirm the cellular uptake. Figure 3 shows the results for NLC-C in the CLSM studies. The upper parts of Fig. 3 show the morphology of MCF-7 cells under white light. We observed that the cell number at the high concentration ($10.4 \mu\text{mol/l}$) was lower than that at the low concentration ($5.2 \mu\text{mol/l}$). Moreover, the control groups presented weak fluorescence (Figs. 3E, G). On the other hand, the NLC-C groups entered breast cancer cells in greater quantities (Figs. 3F, H).

Discussion

In some circumstances, chemotherapeutics for cancer therapy are limited because of MDR. Tryptanthrin is a traditional herbal drug which has seen renewed interest as an indication for regulating gene expression in MDR-associated proteins. However, tryptanthrin is insoluble in biocompatible media, which soluble in DMSO (8 mg/ml) and methanol (0.3 mg/ml). Improving the poor solubility of this drug for delivery into target organs is an important issue which is one of

the key points in the development of pharmaceuticals.¹³ We characterized the drug delivery carriers and determined the feasibility of nanoparticles for delivering tryptanthrin. We found that tryptanthrin-loaded SLNs, NLCs, and LEs overcame the insolubility problem, and allowed tryptanthrin to successfully penetrate breast cancer cells, especially when using the NLC system.

From the aspect of physicochemical properties, we compared the three kinds of nanoparticles: SLNs, NLCs, and LEs. In general, the crystalline lipid core of SLNs produced a larger particle diameter compared to the amorphous core of NLCs. Both Compritol and Precirol are solid lipid material, the backbones of which are derived from glycerides with long alkyl chains. We compared the lengths of the alkyl chains in the two types of solid lipids to derive the physicochemical behavior. In general, we observed that glycerides with longer alkyl chains (Compritol) produced larger particles compared to those with shorter chains (Precirol). In addition, the solid state of NLCs was retained by controlling the liquid lipid content added to the formulation; therefore, controlled drug release properties can be achieved with NLCs.¹⁴ It was proposed that these NLCs are composed of oily droplets embedded in a solid lipid matrix. No special trend in particle size was found for nanoparticles with different Compritol contents. This was basically consistent with the results reported by Jores *et al.*¹⁵ The liquid lipid content did not influence the particle size of NLCs at a liquid lipid content below 25 wt%.^{15,16}

The zeta potential plays an important role in nanoparticle stability due to electrostatic repulsion. The nanoparticle systems of SLNs, NLCs, and LEs were negatively charged in the present study. The origin of the negative charge of the nanoparticles was the anionic fractions of SPC. SPC used as a lipophilic emulsifier in this study contained 80% PC, which

is uncharged. The other components (20%) of SPC are negatively charged, including phosphatidylserine, phosphatidylinositol, phosphatidylethanolamine, phosphatidyl glycerol, and phosphatidic acid.^{17,18)} Moreover, glycerides of fatty acids in the lipid core of Compritol and Precirol contributed to the negative charge. In general, the zeta potentials of all of the various nanoparticles showed no significant differences, and the composition did not influence the negative charge. Measuring the zeta potential allows predictions of the storage stability. Previous studies indicated that particle aggregation is less likely to occur for particles with surface charges of >30 mV.¹⁹⁾

The burst effect is the rapid release of a drug into the blood or organs causing the concentration to quickly rise then briefly plateau. It causes an excess of the drug concentration in the therapeutic range which is usually initially observed, followed by the slow and incomplete release of the drug.²⁰⁾ Moreover, programming the release rate of the drug is an issue of concern in controlled drug delivery systems, since an overdose of a drug can cause serious cytotoxicity in release regions, especially with anticancer drugs. Several studies indicated that SLNs exhibited a burst effect which was attributed to a phase-separation effect in the formulation.¹⁴⁾ In this study, we found no burst effect for either SLNs or NLCs. Some literature describes enrichment of the drug surrounding the core shell when SLN formulations cool down, especially when using the hot homogenization process. According to the results of the partition coefficient, the octanol/water partitioning trend showed that NLCs and LEs were higher than SLNs. The water solubility of tryptanthrin is also low. Therefore, tryptanthrin can be embedded in the inner phase of lipid nanoparticles, followed by its slow release to the external phase. This phenomenon supplies sustained and controlled delivery of the drug. In general, the drug is stably retained in the lipid core, and we determined the external phase in the medium to know the release and calculate the parameters. Zero-order release kinetics was suitable to fit the curve of all lipid nanoparticle with 48 h of administration in this study. This phenomenon indicates that the sustained release of tryptanthrin from all lipid nanoparticles was achieved in this work. Moreover, the incorporation of liquid lipids into the solid lipid matrix caused the NLCs to become more impacted and allowed easier release of the loaded drug, thus increasing the tryptanthrin release rate when liquid lipids were included in the matrix.²¹⁾ Another possibility is that the smaller size of the NLC particles have an increased total surface area. Increased release would therefore be expected. According to the Kevin and Ostwald–Freundlich equation, for small particles, especially in the nanometer range, the saturation solubility significantly increases. Both the increase in the saturation solubility and the enlargement of the surface area contribute to enhancement of the dissolution velocity according to the Noyes–Whitney equation.²²⁾

From the aspect of the different types of nanoparticles, the results present various behaviors.²³⁾ The cell viability results showed that NLCs dose-dependently inhibited MCF-7 cells; in contrast, SLNs did not present the same behavior. A possible contributing reason is that the crystal structures differ between SLNs and NLCs. The NLC structure incorporates liquid lipids into the solid lipid matrix which causes the struc-

ture to be more imperfect and the release more-sustained. Moreover, particle size of the NLCs were smaller than those of the SLNs. Chemical theory mentions that with smaller particle sizes, the surface area is enlarged. Hence, when the particle size is reduced, the cellular uptake ability increases, thus enhancing cytotoxicity.

Past evidence pointed out that the key interaction between cellular membranes and the melting point of the fatty acids in the lipid materials is related to the length of the carbon chain and whether the fatty acid is saturated or unsaturated.²⁴⁾ Hence, we investigated the delivery behavior when incorporating different-length carbon chains in the solid lipid. According to the chemical properties, the melting points of Precirol (C₁₆–C₁₈) and Compritol (C₂₂) are 57 and 68 °C, respectively²⁵⁾; moreover, melting points of NLC systems are generally lower than those of SLN systems. Based on this principle, NLCs incorporating Precirol should present higher cytotoxicity. Our results showed the same phenomena. However, results of the cytotoxicity tests showed highly uptake of SLNs incorporating Precirol than Compritol. These phenomena are counter to this principle. In assessing all of the results, we found that it mostly explained the relative release behavior. NLCs incorporating Compritol exhibited the maximum release percentage of 45% at 48 h; however, it was 36% with Precirol. Hence, the higher drug release produced an increase in the drug concentration which caused the cytotoxicity.

This background on tryptanthrin produced new insights which improved the delivery problems for better chemotherapeutic outcomes. First of all, we tried to employ nanoparticles in this study. In the field of nanotechnology, there are many delivery approaches which focus on the design, characterization, and application of materials at the nano-scale. The present results demonstrated that tryptanthrin-loaded NLCs were taken up by breast cancer cells; moreover, the cytotoxicity encouraged us to further study this. Typically, cancer chemotherapy treatments employ various drug combinations to increase the therapeutic efficacy. Although the approach is usually used in the clinical treatment of cancers, it however can produce unacceptable toxicity thus reducing patient compliance. Recently, several researchers pointed out that tryptanthrin is a potential drug to downregulate the problem of MDR. The concept can hopefully improve chemotherapeutic outcomes in the future. This preliminary study demonstrated the feasibility of tryptanthrin delivery, and MDR remains to be studied further. In the future, our attention will be focused on combining tryptanthrin with anticancer drugs to investigate the manner of the MDR effect.

Conclusion

In summary, the aim of the study was to overcome the insolubility of tryptanthrin and evaluate the feasibility of various lipid nanoparticles including SLNs, NLCs, and LEs. We found that the different compositions of the solid lipid influenced the physicochemical characteristics, partitioning ability, and cytotoxicity in both SLNs and NLCs. Overall, the amorphous core of NLCs produced a smaller particle diameter compared to the crystalline lipid core of SLNs. Moreover, tryptanthrin had a high partitioning affinity in NLC systems. Tryptanthrin loaded in all of the lipid nanoparticles had zero-order kinetics and sustained release properties. The results

demonstrated that the NLC-C formulation is a potential carrier with sustained release behavior and cytotoxicity effects, and allowed tryptanthrin to be taken up by breast cancer cells. From these positive results, we are encouraged to focus on the drug's effects on multidrug resistance.

References

- 1) Gottesman M. M., Fojo T., Bates S. E., *Nat. Rev. Cancer*, **2**, 48—58 (2002).
- 2) Scotto K. W., *Oncogene*, **22**, 7496—7511 (2003).
- 3) Gottesman M.M., Ling V., *FEBS Lett.*, **580**, 998—1009 (2006).
- 4) Yu S. T., Chen T. M., Tseng S. Y., Chen Y. H., *Biochem. Biophys. Res. Commun.*, **358**, 79—84 (2007).
- 5) Jao C. W., Lin W. C., Wu Y. T., Wu P. L., *J. Nat. Prod.*, **71**, 1275—1279 (2008).
- 6) Danz H., Stoyanova S., Wippich P., Brattström A., Hamburger M., *Planta Med.*, **67**, 411—416 (2001).
- 7) Sharma V. M., Prasanna P., Seshu K. V., Renuka B., Rao C. V., Kumar G. S., Narasimhulu C. P., Babu P. A., Puranik R. C., Subramanyam D., Venkateswarlu A., Rajagopal S., Kumar K. B., Rao C. S., Mamidi N. V., Deevi D. S., Ajaykumar R., Rajagopalan R., *Bioorg. Med. Chem. Lett.*, **12**, 2303—2307 (2002).
- 8) Koya-Miyata S., Kimoto T., Micallef M. J., Hino K., Taniguchi M., Ushio S., Iwaki K., Ikeda M., Kurimoto M., *Anticancer Res.*, **21**, 3295—3300 (2001).
- 9) Ogretmen B., Safa A. R., *Biochemistry*, **38**, 2189—2199 (1999).
- 10) Chen G. S., Bhagwat B. V., Liao P. Y., Chen H. T., Lin S. B., Chern J. W., *Bioorg. Med. Chem. Lett.*, **17**, 1769—1772 (2007).
- 11) Jin S., Ye K., *Biotechnol. Prog.*, **23**, 32—41 (2007).
- 12) Müller R. H., Radtke M., Wissing S. A., *Adv. Drug Deliv. Rev.*, **54**, S131—S155 (2002).
- 13) Driscoll D. F., *Pharm. Res.*, **23**, 1959—1969 (2006).
- 14) Müller R. H., Radtke M., Wissing S. A., *Int. J. Pharm.*, **242**, 121—128 (2002).
- 15) Jores K., Haberland A., Wartewig S., Mäder K., Mehnert W., *Pharm. Res.*, **22**, 1887—1897 (2005).
- 16) Hu F. Q., Jiang S. P., Du Y. Z., Yuan H., Ye Y. Q., Zeng S., *Colloids Surface B*, **45**, 167—173 (2005).
- 17) Buszello K., Harnisch S., Müller R.H., Müller B.W., *Eur. J. Pharm. Biopharm.*, **49**, 143—149 (2000).
- 18) Gabizon A., Shmeeda H., Barenholz Y., *Clin. Pharmacokinet.*, **42**, 419—436 (2003).
- 19) Müller R. H., Mäder K., Gohla S., *Eur. J. Pharm. Biopharm.*, **50**, 161—177 (2000).
- 20) Wong H. L., Bendayan R., Rauth A. M., Li Y., Wu X. Y., *Adv. Drug Deliv. Rev.*, **59**, 491—504 (2007).
- 21) Hu F. Q., Jiang S. P., Du Y. Z., Yuan H., Ye Y. Q., Zeng S., *Int. J. Pharm.*, **314**, 83—89 (2006).
- 22) Hou D., Xie C., Huang K., Zhu C., *Biomaterials*, **24**, 1781—1785 (2003).
- 23) Vasir J. K., Reddy M. K., Labhasetwar V. D., *Curr. Nanosci.*, **1**, 47—64 (2005).
- 24) Tranchant T., Besson P., Hoinard C., Delarue J., Antoine J. M., Couet C., Goré J., *Biochim. Biophys. Acta*, **1345**, 151—161 (1997).
- 25) Yuan H., Miao J., Du Y. Z., You J., Hu F. Q., Zeng S., *Int. J. Pharm.*, **348**, 137—145 (2008).